# Au-nanoparticle–bis-bipyridinium cyclophane superstructures: assembly, characterization and sensoric applications

**Michal Lahav, Andrew N. Shipway and Itamar Willner ***

*Institute of Chemistry, The Hebrew University of Jerusalem, Jerusalem 91904, Israel*

***Received (in Cambridge, UK) 7th April 1999, Accepted 30th June 1999***

A three-dimensional conductive superstructure of 12 ± 1 nm Au-nanoparticles was built up on a conductive (indium-doped tin oxide) glass support by means of alternating treatments with Au-nanoparticle and cyclobis(paraquat-*p*-phenylene) tetrachloride solutions. The structure was characterized by absorbance spectroscopy (showing layer build-up and interparticle coupling), and cyclic voltammetry of the gold surface and crosslinking bipyridinium units (showing near-monolayer packing of each nanoparticle layer and a ratio of *ca.* 100 crosslinker molecules for each nanoparticle). The organic crosslinker molecule acts as a receptor for π-donor substrates, thus causing the concentration of such guests at the conductive superstructured array. This effect facilitates the use of the electrode as an effective sensing matrix for *p*-hydroquinone, 3,4-dihydroxyphenylacetic acid, dopamine and adrenaline, to concentrations as low as 1 μM. The sensitivity of the nanostructured array is controlled by the number of receptor/Au-nanoparticle layers associated with the electrode. Control experiments reveal that the superstructured electrode exhibits selectivity which is a consequence of specific interactions between the guests and the receptor, rather than the result of surface area or microenvironmental effects.

## Introduction

The chemical modification of surfaces with functionalized monolayers or thin films attracts extensive research efforts directed towards the miniaturization of devices and the tailoring of nanoscale composite assemblies with unique electronic and photonic functions.[1] The functionalization of electrodes with ordered molecular redox-active components has yielded assemblies revealing vectorial electron transfer[2] and sensoric activities such as pH-sensors.[3] The functionalization of solid supports (*e.g.* piezoelectric crystals or electrodes) with monolayers consisting of molecular receptor units[4] or oligonucleotides[5] has enabled the analysis of the formation of complementary recognition or affinity complexes at the sensing interfaces. Modification of electrodes with photoisomerizable, redox-activated monolayers or thin films[6] has been reported to stimulate the electronic transduction of recorded optical information, while the functionalization of conductive supports with photoisomerizable monolayers[7] yields photocommand surfaces for controlling interfacial electron transfer. Similarly, photoactive monolayers or thin films have been used to generate patterned micro-domains of controllable physical or chemical functionality.[8]

Nanoparticles and functionalized nanoparticles are extensively studied because of their unique optical,[9] photocatalytic,[10] electronic,[11] and catalytic[12] functions. The assembly of nanoparticles on solid supports is expected to yield systems of unique photonic and electronic properties. Au- or Ag-colloid monolayers can be assembled on glass or conductive glass supports by the self-organization of the metal particles onto aminosiloxane or thiolsiloxane layers associated with the solid supports.[13–15] Enhanced resonance Raman spectroscopy of molecular adsorbates,[13] and high-surface area roughened surfaces for electrochemical processes,[15] have been reported for these colloid monolayers. Au- or Ag-nanoparticles, or Au–Ag composite arrays, have been constructed by the use of dithiols[16] or diaminobipyridinium[17] as molecular crosslinkers. Similarly, layered polyelectrolyte–Au-nanoparticle arrays have been assembled on surfaces.[18] Recently, interest has grown in the nanometer-scale organization of metal colloids for the assembly of nano-devices. $Au_{55}$-clusters have been reported to act as a tunnel resonance resistor[19] and an Au-cluster was used as a single electron tunneling transistor.[20] A Zn(II)-porphyrin–viologen dyad was used to crosslink Au-nanoparticles, and the resulting array was employed as the active interface in a photoelectrochemical cell.[21]

In another study,[22] we reported on the assembly of a three-dimensional Au-superstructure crosslinked by a bipyridinium cyclophane and assembled on a conductive ITO surface. It was demonstrated that the Au-superstructure exhibits lateral conductivity, and that the bipyridinium cyclophane 'glue molecules' act as receptor sites for the electrochemical sensing of hydroquinone. Enhanced sensitivity for the sensing of hydroquinone was observed, as a result of the concentration of the analyte in the receptors' binding sites. In this paper we address in detail the characterization of the three-dimensional Au-nanoparticle array, and discuss the application of the assembly for the electrochemical sensing of various π-donor substrates, and specifically neurotransmitters, *e.g.* dopamine, dihydroxyphenylacetic acid, adrenaline.

## Experimental

### Materials

Cyclobis(paraquat-*p*-phenylene) † tetrachloride was synthesized according to the literature.[23] 12 ± 1 nm Au-colloids were synthesized[24] by the addition of $AuHCl_4 \cdot 3H_2O$ (50 mg) to a rapidly stirring, refluxing solution of sodium citrate (100 mg) in water (500 mL), which was then stirred under reflux for a further 15 min before being allowed to cool. Ultrapure water was used throughout this work and was obtained from a nanopure system (Barnstead). All other materials (Aldrich) were used with no further purification.

### Electrode modifications

All electrodes were indium-doped tin oxide (ITO) coated (both sides) glass cut to 10 × 20 mm. Cleaning and silylation of the electrodes were performed according to the literature.[15] The electrodes were washed with ethanol, sonicated for 15 min in 5% HCl, washed with ethanol, and then with water. Silylation was performed by immersion in a 2–3% solution of 3-aminopropyl-

† Paraquat is 1,1′-dimethyl-4,4′-bipyridinium.

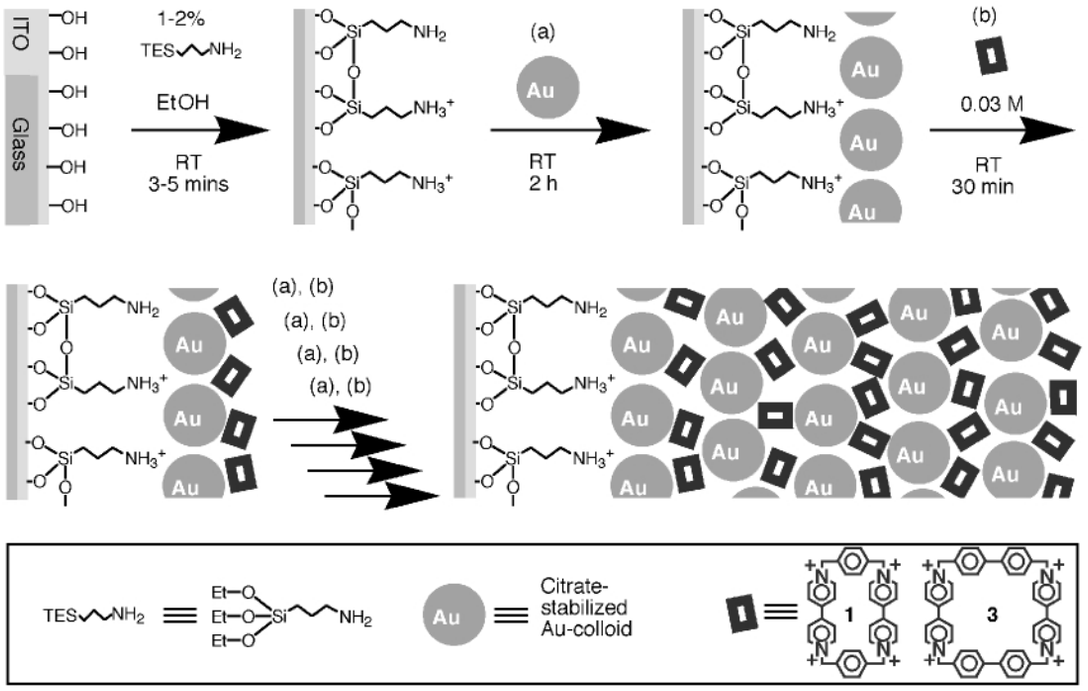


**Scheme 1** The stepwise assembly of the three-dimensional array of the bis-bipyridinium cyclophane and Au-nanoparticles on a conductive ITO support.

triethoxysilane for *ca.* 2 min, after which the electrodes were washed thoroughly with ethanol, and were then heated to 110 °C for 10 min. Finally, the silylated electrodes were washed with water. Colloid treatment of electrodes consisted of immersion in the colloid solution for 2 h, and cyclophane treatment with immersion in a *ca.* 30 mM solution of the cyclophane tetrachloride for 30 min. After each treatment, the electrode was washed three times with water. Special attention was paid to avoid the drying of the electrode. The electrodes were stored in water, and during electrochemical measurements the lower 3–5 mm of the electrodes were immersed in the electrochemical cell.

### Instrumentation

Absorbance spectra were measured on a Uvikon 860 (Kontron) spectrophotometer, and the pHs of buffer solutions with a pH-meter (Corning ion analyzer 150). Transmission Electron Micrographs (TEM) were obtained on a Jeol 100 CX. 300 Mesh carbon/formvar-coated grids were pretreated by the evaporation of a drop of aqueous 3-aminopropyltriethoxysilane (1 ppm), and were then washed with water. The sample was deposited on the grid by interaction for 10 minutes, followed by washing with water to remove any unbound particles. Electrochemical measurements were performed using a potentiostat (EG&G, Versastat) connected to a personal computer (EG&G). All measurements were carried out at ambient temperature (25 ± 3 °C) in a three compartment electrochemical cell consisting of the chemically modified electrode as the working electrode, a glassy carbon auxiliary electrode isolated by a glass frit, and a saturated calomel electrode (SCE) connected to the working volume with a Luggin capillary. All potentials are reported with respect to the SCE. Argon bubbling was used to remove oxygen from the electrolyte solutions in the electrochemical cell.

## Results and discussion

The Au-nanoparticle/cyclobis(paraquat-*p*-phenylene) (bipyridinium cyclophane **1**) superstructure was assembled as outlined in Scheme 1. An ITO conductive glass support was first functionalized with an aminopropylsiloxane film. The resulting functionalized support was then interacted with a citrate-stabilized Au-nanoparticle suspension (diameter 12 ± 1 nm) to yield a self-assembled metal colloid layer. The resulting interface was treated with cyclobis(paraquat-*p*-phenylene) (**1**) and then again with the Au-colloid. By the repeated interaction of the electrode with **1,** and then with the gold nanoparticles, an array with a controllable number of Au-layers could be generated.

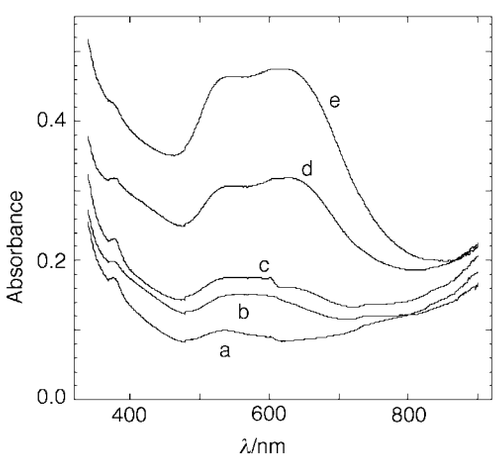


**Fig. 1** Absorbance spectra of the layered receptor–Au-colloid superstructure: (a) one Au-layer (b) two Au-layers (c) three Au-layers (d) four Au-layers (e) five Au-layers.

The formation of the Au-colloid was supported by spectroscopic and electrochemical means. Fig. 1 shows the absorption spectra of the Au-colloid superstructures upon the build-up of the particle layers. The characteristic Au-plasmon absorbance at $\lambda = ca.$ 520 nm increases in intensity with number of layers. It is also observed that with the increase of the number of layers, a second absorbance band at $\lambda = ca.$ 650 nm is formed, which is strengthened and is bathochromically shifted as the number of Au-particle layers increases. This absorbance has been attributed to exitonic transitions caused by interparticle plasmon coupling, a phenomenon which emerges at interparticle

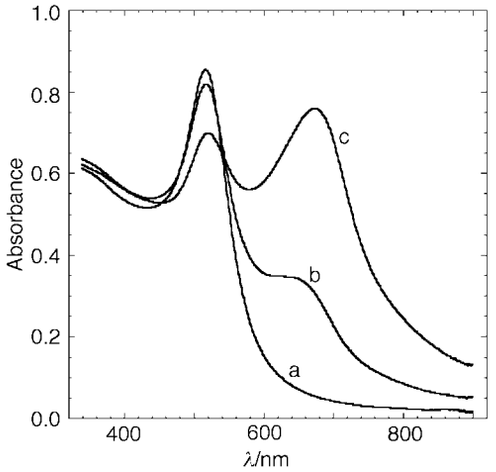


**Fig. 2** Absorbance spectra of Au-nanoparticle suspensions 15 min after the addition of various quantities of cyclobis(paraquat-*p*-phenylene): (a) without any addition (b) after the addition of (an average of) 50 molecules of **1** per Au particle (c) after the addition of 100 molecules of **1** per Au particle.

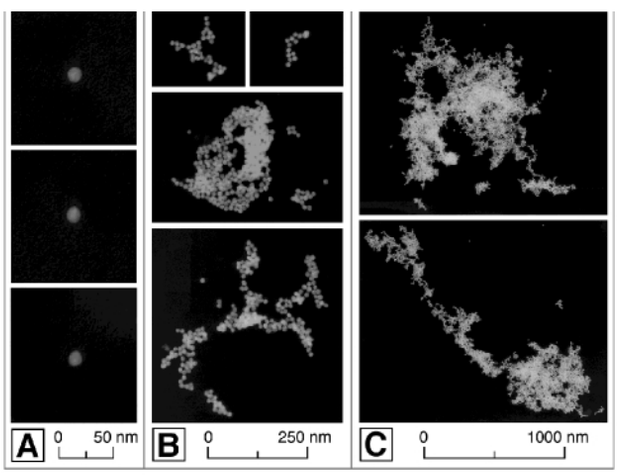


**Fig. 3** Representative aggregates of Au-nanoparticles observed in the transmission electron micrographs of amine-functionalized grids treated with Au-colloid suspensions to which various quantities of cyclobis(paraquat-*p*-phenylene) have been added: (A) without any addition (B) after the addition of 50 molecules per Au particle (C) after the addition of 100 molecules per Au particle.

spacings below 5 nm.[25] Thus, the bipyridinium cyclophane (**1**) acts as a molecular crosslinker of the Au-particles. Further evidence that these absorbance changes occur as a result of the aggregation of Au-nanostructures is obtained by following the spectral changes of a citrate-stabilized Au-nanoparticle solution upon the addition of **1**. Fig. 2 shows the spectral changes of the sample upon the addition of various quantities of **1**. Upon the addition of a small amount of **1**, the intensity of the plasmon absorbance at 520 nm is reduced and a band at $\lambda = ca.$ 650 nm, similar to the spectra observed with superstructure growth on the surface, is formed. As more cyclophane is added, this absorbance intensifies at the expense of the plasmon absorbance of individual particles ($\lambda = ca.$ 520 nm). After longer interaction times (2 h) of the Au-particles with **1**, at a concentration of at least 100 molecules per colloid particle, the solution turns turbid and the particles ultimately precipitate. Fig. 3 shows electron micrographs of colloid suspensions after interaction with cyclophane **1** at concentrations of 0, 50, and 100 molecules per particle, for 15 min. With no interaction, only single particles are observed (Fig. 3(A)), but as the aggregating agent is added in larger concentrations, clusters and aggregates become prominent (Fig. 3 (B and C)). Further association of these multiparticle structures causes the eventual precipitation of the Au nanoparticles.

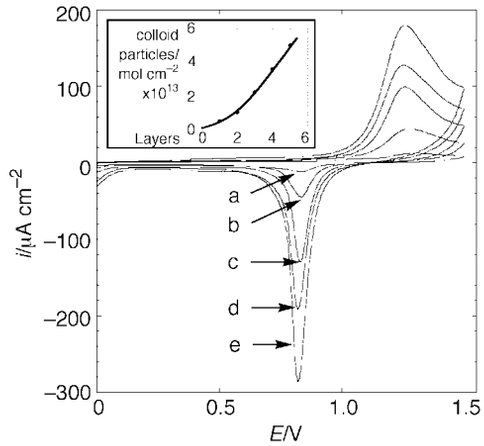


**Fig. 4** Cyclic voltammograms of the layered Au-colloid assemblies corresponding to the electrochemical oxidation and reduction of the particle surface: (a) to (e) correspond to one up to five layers of Au-particles. Experiments were carried out in 1.0 M $H_2SO_4$, scan rate 50 mV $s^{-1}$. Inset: Calibration curve corresponding to the surface coverage of Au-nanoparticles against number of layers (extracted by coulometric analysis of the gold oxide reduction peak).

Fig. 4 shows cyclic voltammograms of the Au-colloid layered array upon construction of the superstructure. The characteristic cyclic voltammogram of Au is observed, consisting of an oxidative wave corresponding to the formation of the Au-oxide layer on the colloid particles, followed by a wave corresponding to the reduction of the oxide layer. The cyclic voltammograms increase almost linearly except for the first layer, which reveals a lower content of Au-particles. This lower content of the Au-nanoparticles in the base layer is attributed to the inefficient aminopropylsiloxane functionalization of the ITO surface, leading to the incomplete coverage of the surface with the gold particles. The build-up of the second layer onwards, where the Au-nanoparticles are crosslinked by **1**, exhibits a dense configuration. By the coulometric assay of the reduction wave of the Au-particles, the total gold area per layer can be estimated. Knowing the diameter of the Au-particles, and assuming that all of the particle surface is exposed to the electrochemical reaction, we estimate the lower limit of the surface density of Au-particles to be $0.8 \times 10^{11}$ particles $cm^{-2}$ per layer. This value is in excellent agreement with the surface coverage value determined by AFM for a single Au-particle layer on the base aminosiloxane matrix ($1 \times 10^{11}$ particles $cm^{-2}$).[26]

As cyclobis(paraquat-*p*-phenylene) (**1**) is electroactive, the increase in the electrochemical response of the molecular crosslinker could reflect the build-up and formation of the particle superstructure. Fig. 5 shows the cyclic voltammograms of the molecular crosslinking units upon formation of the layered array. The cyclic voltammogram of **1** increases as the number of Au-layers is raised. This implies that **1** indeed acts as molecular crosslinking 'glue' for the particles, and that the formation of each additional Au-layer requires the pre-assembly of the cyclophane. By the coulometric analysis of the electrical responses of **1** upon the build-up of the array, we estimate the content of **1** to be $1.5 \times 10^{-11}$ moles $cm^{-2}$ per layer (Fig. 5, inset). Knowing the surface coverage of the Au-particles, we estimate that *ca.* 100 crosslinking molecules of **1** are associated with each Au-particle in the superstructure, a value that is in excellent agreement with the estimated number required to precipitate Au-colloid from solution (*vide supra*). Thus, the formation of the nanoparticle array may be attributed to electrostatic attraction between the positively-charged crosslinker (**1**) and the negatively-charged citrate-stabilized particles. The fact that the molecular crosslinker **1** is electrochemically observable upon the build-up of the superstructure implies that the array exhibits three-dimensional conductivity. It should be noted that the **1**-crosslinked Au-particle structures exhibit high

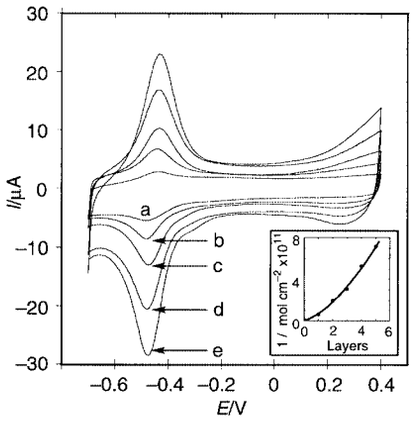


**Fig. 5** Cyclic voltammograms corresponding to the redox activity of the crosslinker (**1**) in arrays of different numbers of layers: (a) to (e) correspond to one up to five layers of Au-particles. Experiments were recorded under argon in 0.1 M phosphate buffer solution, pH = 7.2, scan rate 100 mV $s^{-1}$. Inset: Calibration curve corresponding to the surface coverage of **1** against number of layers as extracted by coulometric analysis of the curves.

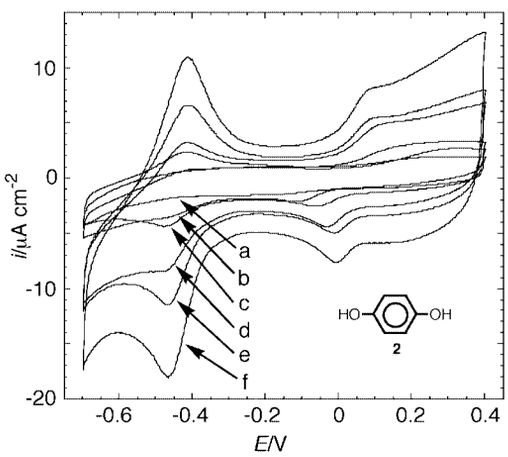


**Fig. 6** Cyclic voltammograms of the layered **1**–Au-colloid arrays in the presence of hydroquinone (**2**) $1 \times 10^{-5}$ M. (a) ITO electrode modified only with a layer of Au-colloid. (b) to (f) One to five Au-nanoparticle layers. All data were recorded under argon in 0.1 M phosphate buffer solution, pH = 7.2, scan rate 100 mV $s^{-1}$.

stability. Introduction of the modified surfaces into a buffer solution does not affect the superstructure properties, and only physical scratching removes the Au-particles from the ITO surface.

Cyclobis(paraquat-*p*-phenylene) (**1**) acts as a π-acceptor receptor for the complexation of π-donor substrates such as dialkoxybenzene derivatives and hydroquinone substrates.[27] Accordingly, we envisaged that **1**–Au-particle arrays assembled onto the ITO conductive glass could act as electrochemical sensing interfaces for hydroquinone derivatives as a result of the preconcentration of the substrate by the organized array. The three-dimensional conductivity of the superstructure, together with the redox-activity of hydroquinones, implies that electrochemical sensing of these substrates is feasible. Furthermore, the fact that a controllable number of receptor–Au-particle layers can be assembled on the conductive support suggests that interfaces for hydroquinones of tunable sensitivity can be tailored. Fig. 6 shows the cyclic voltammograms of ITO electrodes that are modified with various numbers of **1**-receptor and Au-particle layers in the presence of *p*-hydroquinone (**2**) at $1 \times 10^{-5}$ M. No electrochemical response for **2** is observed at the ITO electrode that was modified only by a single layer of Au-colloid due to the low bulk-concentration of the hydroquinone in the electrolyte solution. The hydroquinone is, however, detected electrochemically, ($E^\circ = 0.02$ V *vs.* SCE at pH = 7.2), in the presence of the **1**–Au-colloid arrays. The electrochemical responses of **2** increase as the number of **1**–Au-particle layers increases. This is consistent with the improved preconcentration of **2,** at the nanostructured array, by the receptor units that generate surface-associated π-donor–acceptor complexes between **1** and **2**. As the surface coverage of **1** in the array increases, enhanced preconcentration of **2** at the conductive support occurs. In addition, the electrochemical response of hydroquinone (**2**) is further enhanced by a dramatic decrease in the peak-to-peak separation of its redox wave as the number of layers increases, implying improved interfacial electron-transfer kinetics upon the buildup of layers.

Several additional control experiments were performed in order to elucidate the nature of the binding interactions between **2** and the particle array. It is still possible that non-specific interactions between **2** and the cyclophane/Au array lead to the association of **2** to the matrix. Furthermore, the build-up of the Au-nanoparticle array increases the surface area of the conductive support, which could account for the enhanced amperometric response of *p*-hydroquinone (rather than the host–guest interaction that we propose). To address these issues, a related nanostructured array consisting of *N*,*N*′-diaminoethyl-4,4′-bipyridinium and Au-particles was constructed.[17] It is well established that the bipyridinium cyclophane **1** exhibits a substantially higher affinity for π-donor substrates as compared to the single *N*,*N*′-dialkyl-4,4′-bipyridinium constituent. This originates from the possibility of intercalating the π-donor between the two π-acceptor sites of **1**. Indeed, interaction of **2**, $1 \times 10^{-5}$ M, with an *N*,*N*′-dialkyl-4,4′-bipyridinium-crosslinked Au-array (5 layers) does not yield any noticeable electrochemical response for *p*-hydroquinone. These results indicate that neither the increased surface area of the electrode nor non-specific interactions are the origin of the electrochemical sensitivity for sensing **2**, and that the electrochemical responses of **2** in the presence of the bipyridinium cyclophane/Au-colloid arrays originate from the formation of specific π-donor–acceptor complexes between the analyte and the crosslinking receptor sites. The porosity of the assembly and the possible shielding of **1** towards **2** by the Au-particles were also examined (Scheme 2): *p*-hydroquinone was sensed by

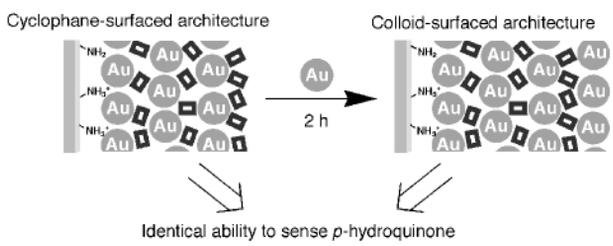


**Scheme 2** Schematic demonstration of the porosity of the multilayered receptor–nanoparticle architecture to molecular analytes.

a 3-layer cyclophane–colloid assembly (of which the final treatment was with the cyclophane component). A fourth layer of Au-particles was then assembled onto the same electrode, and **2** was reanalyzed. In the first electrode configuration, **1** is exposed to the analyte solution, whereas in the latter electrode structure, all receptor sites are shielded by the Au-particles. We find that the electrical response of **2** is identical in the two electrode configurations. This clearly indicates that **1** is similarly accessible by the two crosslinking receptor configurations, implying that the Au-particle array is indeed porous.

A five-layer **1**–Au-nanoparticle assembly was used to sense *p*-hydroquinone (**2**) at different concentrations. Fig. 7 shows the cyclic voltammograms acquired. As the bulk concentration of **2** increases, its amperometric response is enhanced. Fig. 7, inset, shows the derived calibration curve corresponding to the coulometric analysis of the electrochemical response of **2** at different bulk concentrations. The crosslinked Au-nanoparticle-

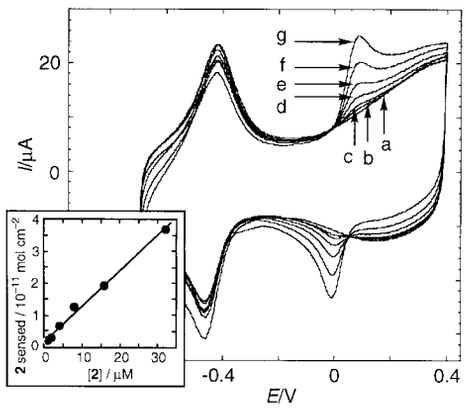


**Fig. 7** Cyclic voltammograms of a layered bis-bipyridinium–Au-nanoparticle array (five layers) in the absence of *p*-hydroquinone (curve a) and in various concentrations of *p*-hydroquinone, (**2**); (b) $1 \times 10^{-6}$ M; (c) $2 \times 10^{-6}$ M; (d) $4 \times 10^{-6}$ M; (e) $8 \times 10^{-6}$ M; (f) $1.6 \times 10^{-5}$ M; (g) $3.2 \times 10^{-5}$ M. Inset: Calibration curve corresponding to the electrochemical sensing of (**2**). All data were recorded under argon in 0.1 M phosphate buffer, pH = 7.2, scan rate 100 mV $s^{-1}$.

functionalized electrodes are stable and reusable sensing interfaces for at least two weeks for the analysis of *p*-hydroquinone (**2**) and the other hydroquinone derivatives described in the present study (*vide infra*). The hydroquinones associated with the sensing interface can be washed off by immersion in a pure phosphate buffer solution, regenerating the sensing interface.

The selectivity of the array is a major issue. In order to assess the selectivity of the **1**–Au-nanoparticle array for hydroquinones over other substrates, we attempted to use the array to sense dihydroxymethylferrocene. No electrochemical response for this π-donor could be detected, presumably because it is too large to be bound by the cyclophane **1**. Construction of an Au-nanoparticle superstructure with the enlarged cyclophane cyclobis(paraquat-*p*-biphenylene) (**3**), however, yields an array that is capable of sensing dihydroxymethylferrocene, but not *p*-hydroquinone.[28] Clearly, the receptor–Au-nanoparticle superstructures reveal substrate selectivity based on the 'fit' of the analyte in the cavity of the cyclophane.

Similarly, 3,4-dihydroxyphenylacetic acid (**4**) was analyzed by the bipyridinium cyclophane-crosslinked Au-particle array. Fig. 8(A) shows the cyclic voltammograms of ITO supports functionalized by different numbers of crosslinked Au-layers in the presence of **4**. The electrochemical response of **4** at $E^\circ = 0.10$ V *vs*. SCE at pH = 7.2 rises as the number of Au-layers increases. Since **4** is negatively-charged at pH = 7, its electrostatic attraction by the bipyridinium cyclophane sites could lead to its concentration at the electrode support, and thereby to the resulting electrical response. To address this possibility, we used an ITO glass modified by five layers of the Au-colloid and crosslinked by the unimolecular *N*,*N*′-diaminoethyl-4,4′-bipyridinium 'molecular glue'. No significant electrical response for **4** could be detected in the presence of this Au-array, implying that electrostatic interactions do not play an important role in the concentration of **4** at the electrode. We thus conclude that concentration of **4** at the conductive support originates from π-donor–acceptor interactions between **4** and the bis-bipyridinium cyclophane receptor sites. The cyclic voltammograms of a five-layer Au-colloid array in the presence of different concentrations of **4** are shown in Fig. 8(B). As the concentration of **4** increases, its amperometric response is enhanced, allowing us to derive the respective calibration curve (Fig. 8(B), inset).

The potential of the **1**-crosslinked Au-nanoparticle superstructure for practical sensing applications is of particular interest. Several neurotransmitters include the *o*-hydroquinone moiety, and thus they may feasibly be sensed by their concentration in the **1**–Au-nanoparticle array. Accordingly, cyclobis-(paraquat-*p*-phenylene)–Au-particle array was also used to

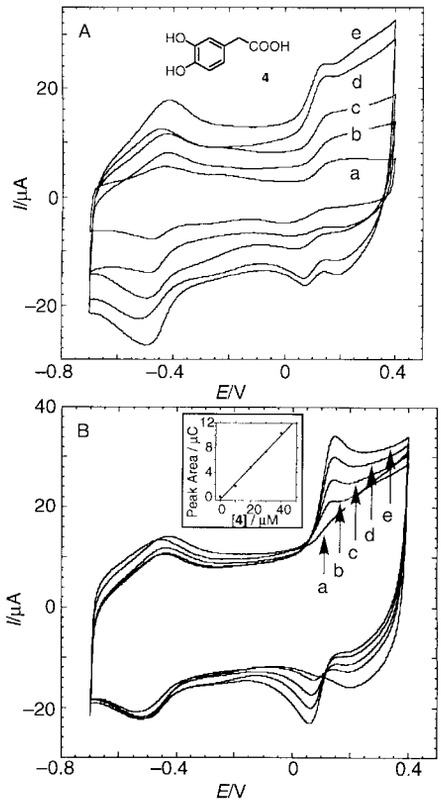


**Fig. 8** (A) Cyclic voltammograms of the layered **1**–Au-colloid arrays in the presence of 3,4-dihydroxyphenylacetic acid (**4**) $1 \times 10^{-5}$ M. (a) to (e) One to five Au-nanoparticle layers. (B) Cyclic voltammograms of a 5-layer electrode in the presence of various concentrations of **4**; (a) 0 M; (b) $10 \times 10^{-6}$ M; (c) $20 \times 10^{-6}$ M; (d) $30 \times 10^{-6}$ M; (e) $40 \times 10^{-6}$ M. Inset: Calibration curve corresponding to the electrochemical sensing of **4** by the analysis of the peak current of the substrate's redox wave (at $E^\circ = 0.18$ V *vs*. SCE). All data were recorded under argon in 0.1 M phosphate buffer solution, pH = 7.2, scan rate 100 mV $s^{-1}$.

electrochemically sense a series of neurotransmitters, *e.g.* dopamine (**5**) and adrenaline (**6**). These substrates contain π-donor *o*-hydroquinone units, but in addition include β-aminoalkyl substituents on the aromatic ring. The common structure of these compounds leads to common electrochemical behavior. The electrochemistry of these compounds has been examined and discussed in homogeneous aqueous solution,[29] and is summarized in Scheme 3. Oxidation of the *o*-hydroquinone residue to the respective quinone (**I**) is only partly reversible since the amine substituent induces a Michael addition accompanied by a ring-closure and the formation of intermediate **II**, exhibiting reversible or quasi-reversible electrochemical properties. Fig. 9(A) shows the second scanned cycles of cyclic voltammograms of dopamine (**5**) ($1 \times 10^{-5}$ M) in the presence of ITO electrodes functionalized with different numbers of crosslinked Au-layers. In addition to the redox wave corresponding to the bipyridinium crosslinker at $E^\circ = -0.44$ V *vs*. SCE, two additional quasi-reversible redox waves at $E^\circ = -0.25$ V and 0.3 V *vs*. SCE are observed. The amperometric responses and the charge associated with these waves increase with the number of layers. No electrical response for dopamine (**5**) at a bulk concentration of $1 \times 10^{-5}$ M could be detected either at a bare ITO electrode or at a 5-layer electrode crosslinked by *N*,*N*′-diaminoethyl-4,4′-bipyridinium,[17] suggesting that the response for **5** at the cyclophane-crosslinked electrode results from the binding of the the analyte to the receptor **1**. The enhanced local concentration of **5** at the nanostructured surface yields the observed electrical response. As previously noted, the cyclic voltammograms shown in Fig. 9(A) represent the second scanned cycle. In the first cycle, the redox wave at

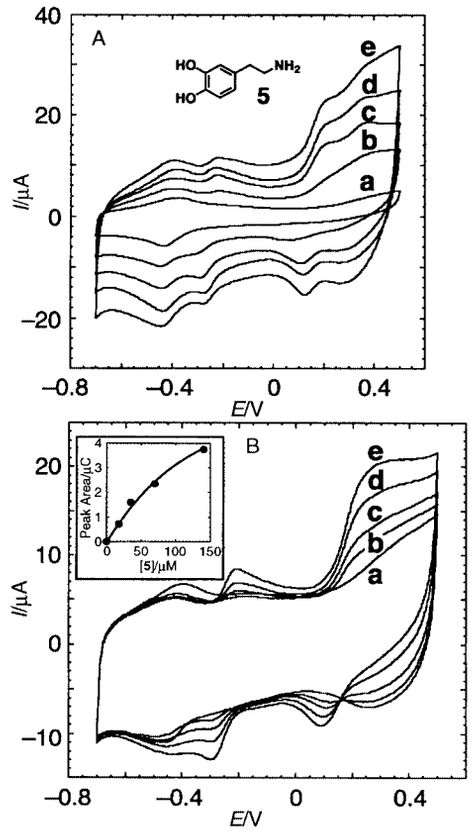


**Fig. 9** (A) Cyclic voltammograms of the layered **1**–Au-colloid arrays in the presence of dopamine (**5**) $1 \times 10^{-5}$ M. (a) to (e) One to five Au-nanoparticle layers. (B) Cyclic voltammograms of a 5-layer electrode in various concentrations of **5**; (a) 0 M; (b) $17 \times 10^{-6}$ M; (c) $35 \times 10^{-6}$ M; (d) $70 \times 10^{-6}$ M; (e) $140 \times 10^{-6}$ M. Inset: Calibration curve corresponding to the electrochemical sensing of **5** by the analysis of the oxidation peak of the product of the electrocatalyzed Michael-type cyclization of **5** (at $E^\circ = -0.20$ V *vs.* SCE). All data were recorded under argon in 0.1 M phosphate buffer solution, pH = 7.2, scan rate 100 mV $s^{-1}$.

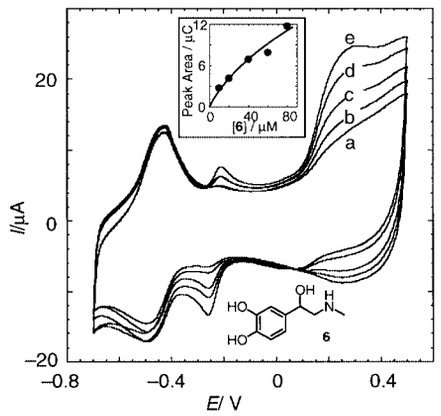


**Fig. 10** Cyclic voltammograms of a 5-layer electrode in various concentrations of adrenaline (**6**); (a) $10 \times 10^{-6}$ M; (b) $20 \times 10^{-6}$ M; (c) $40 \times 10^{-6}$ M; (d) $60 \times 10^{-6}$ M; (e) $80 \times 10^{-6}$ M. Inset: Calibration curve corresponding to the electrochemical sensing of **6** by the analysis of the reduction peak of the product of the electrocatalyzed Michael-type cyclization of **6** (at $E^\circ = -0.26$ V *vs.* SCE). All data were recorded under argon in 0.1 M phosphate buffer solution, pH = 7.2, scan rate 100 mV $s^{-1}$.

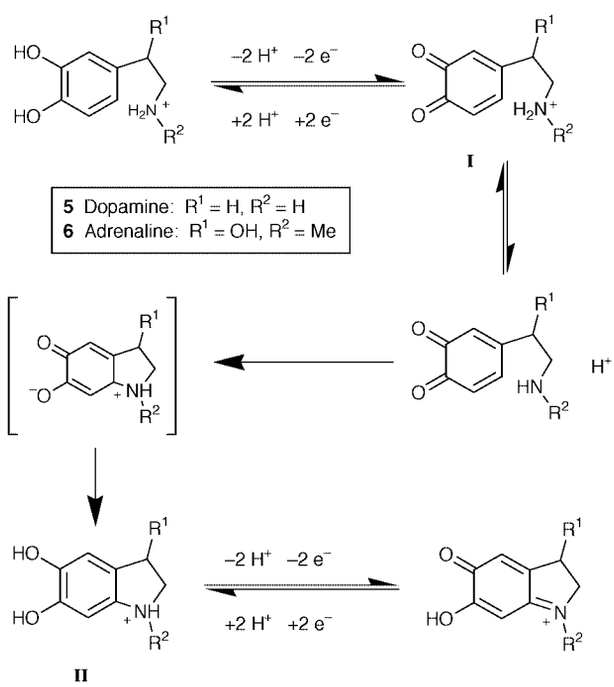


**Scheme 3** Electrochemical transformation of 4-(β-aminoalkyl)-1,2-benzohydroquinones.

$E^\circ = -0.25$ V is not observed and the anodic wave at 0.3 V is broader and of greater intensity. The former wave is only observed after the oxidation of **5** takes place, initiating the Michael-type ring closing reaction (Scheme 3). It is the product of this reaction that is responsible for the reduction wave at $E^\circ = -0.25$ V in the second cycle. This product (species **II** in Scheme 3) is also a superior π-donor to the starting material, and as a result may remain preferentially bound in the matrix, accounting for its high electrochemical visibility and allowing it to be used as a probe for the bulk concentration of **5**. Fig. 9(B) shows the cyclic voltammograms (second scanned cycles) for an ITO electrode consisting of five Au-layers at different concentrations of **5**. The oxidation waves (*ca.* 0.3 V *vs.* SCE) as well as the reversible redox wave of the secondary product increase as the bulk of concentration of **5** is elevated. It is difficult to derive coulometric data from the ill-defined wave for the oxidation of **5**, but the reversible redox-wave corresponding to the secondary product can be used to derive the respective calibration curve, Fig. 9(B), inset. Similar results are obtained for adrenaline (**6**). Fig. 10 shows the cyclic voltammograms of ITO electrodes (second scanned cycles) modified by five layers of **1**-crosslinked Au-particles at different concentrations of **6**. In addition to the constant redox wave at $E^\circ = -0.46$ V *vs.* SCE (corresponding to the cyclophane crosslinker), two other waves are observed: a quasireversible redox wave at −0.28 V, and an irreversible oxidation wave at 0.3 V *vs.* SCE. The quasireversible wave is only observed in the second cycle, supporting its assignment as the response of the secondary product formed by a Michael-type cyclization after the oxidation of **6**. The irreversible oxidation wave at 0.3 V is therefore attributed to the oxidation of **6** and the formation of species **I** (Scheme 3). The reduction of the electrogenerated quinone is barely visible since the subsequent Michael addition is fast. The irreversible oxidation waves corresponding to the oxidation of **6** (Fig. 10), as well as the reversible redox-waves of the electrogenerated product, increase as the bulk concentration of **6** is elevated. Using the reversible wave as a probe, we derived the appropriate calibration curve for the sensing of **6**, (Fig. 10, inset). It should be noted that within this concentration range, adrenaline (**6**) could not be sensed by either a bare ITO electrode or a 5-layer electrode crosslinked by *N*,*N*′-diaminomethyl-4,4′-bipyridinium, verifying that its observed electrochemical sensing originates from its association with the cyclophane **1**. Also the substrates **5**, **6** are positively-charged at pH = 7.2, so even though the substrates are electrostatically repelled by the cyclophane receptor, their concentration at the crosslinked Au-superstructure occurs.

In all of the systems that were studied, the sensing electrodes can be regenerated and reused by their rinsing with a phosphate

buffer solution. In the present study we prepared for each analyte new sets of nano-structured Au-electrodes. We find excellent reproducibility in the formation of the functionalized conductive supports.

## Conclusions

We have presented a novel approach to tailoring superstructures of Au-nanoparticles crosslinked by the molecular π-acceptor cyclobis(paraquat-*p*-phenylene) (**1**), acting as a 'molecular glue' for the metal particles, and as a receptor for π-donor substrates. We have demonstrated that the crosslinked Au-particle array exhibits high porosity for molecular substrates and three-dimensional conductivity. This enables the organization of selective electrochemical sensing interfaces of tunable sensitivity. We have demonstrated that the binding of various hydroquinone substrates to the receptor sites together with the three-dimensional conductivity of the array enables the enhanced electrochemical sensing of the substrates.

## Acknowledgements

This study was supported by the Israel Science Foundation founded by The Israel Academy of Science. A. N. Shipway acknowledges a postdoctoral fellowship from the Royal Society (UK).

## References

1 (*a*) K. E. Drexler, Ed., *Nanosystems*, *Molecular Machinery*, *Manufacturing and Computation*, Wiley, New York, 1992; (*b*) J.-M. Lehn, *Angew. Chem.*, *Int. Ed. Engl.*, 1990, **29**, 1347; (*c*) P. Ball, *Nature*, 1993, **362**, 123; (*d*) F. L. Carter, R. E. Siatowsky and H. Woltjien, Eds., *Molecular Electronic Devices*, Elsevier, Amsterdam, 1988.
2 (*a*) T. Parpaleix, J.-M. Laval, M. Majda and C. Bourdillon, *Anal. Chem.*, 1992, **64**, 641; (*b*) A. Doron, M. Portnoy, M. Lion-Dagan, E. Katz and I. Willner, *J. Am. Chem. Soc.*, 1996, **118**, 8937; (*c*) E. Katz, V. Heleg-Shabtai, I. Willner, H. K. Rau and W. Haehnel, *Angew. Chem.*, *Int. Ed. Engl.*, 1998, **37**, 3253.
3 J. J. Hickman, D. Ofer, P. E. Laibinis, G. M. Whitesides and M. S. Wrighton, *Science*, 1991, **252**, 688.
4 (*a*) K. D. Schierbaum, T. Weiss, E. U. Thorden van Zelzen, J. F. G. Engbersen, D. N. Reinhoudt and W. Göpel, *Science*, 1994, **265**, 1413; (*b*) I. Rubenstein, S. Steinberg, Y. Tor, A. Shanzer and J. Sagiv, *Nature*, 1988, **332**, 426.
5 (*a*) A. Bardea, A. Dagan, I. Ben-Dov, B. Amit and I. Willner, *Chem. Commun.*, 1998, 1393; (*b*) K. Niikura, H. Matsuno and Y. Okahata, *J. Am. Chem. Soc.*, 1998, **120**, 8537; (*c*) Y. Okahata, K. Niikura, Y. Sugiura, M. Sawada and T. Morii, *Biochemistry*, 1998, **37**, 5666.
6 (*a*) J. Daub, J. Salbeck, T. Knöchel, C. Fisher, H. Kunley and K. M. Rapp, *Angew. Chem.*, *Int. Ed. Engl.*, 1989, **28**, 1494; (*b*) I. Willner, M. Lion-Dagan, S. Marx-Tibbon and E. Katz, *J. Am. Chem. Soc.*, 1995, **117**, 6581; (*c*) A. Doron, E. Katz, M. Portnoy and I. Willner, *Angew. Chem.*, *Int. Ed. Engl.*, 1996, **35**, 1535; (*d*) I. Willner, R. Blonder, E. Katz, A. Stocker and A. F. Bückmann, *J. Am. Chem. Soc.*, 1996, **118**, 5310; (*e*) I. Willner, A. Doron and E. Katz, *J. Phys. Org. Chem.*, 1998, **11**, 546; (*f*) I. Willner and B. Willner, *J. Mater. Chem.*, 1998, **8**, 2543.
7 A. Doron, E. Katz, G. Tao and I. Willner, *Langmuir*, 1997, **13**, 1783.
8 (*a*) J. M. Calvert, *J. Vac. Sci. Technol. B*, 1993, **11**, 2155; (*b*) G. Sundarababu, H. Gao and H. Sigrist, *Photochem. Photobiol.*, 1995, **61**, 540; (*c*) T. Matsuda and T. Suguwara, *Langmuir*, 1995, **11**, 2267; (*d*) M. Yan, S. X. Lai, M. N. Wybourne and J. F. W. Keana, *J. Am. Chem. Soc.*, 1993, **115**, 814; (*e*) D. J. Pritchard, H. Morgan and J. M. Cooper, *Angew. Chem.*, *Int. Ed. Engl.*, 1995, **34**, 91; (*f*) M. Hengsakul and A. E. G. Cass, *Bioconjugate Chem.*, 1996, **7**, 249.
9 (*a*) P. Mulvaney, *Langmuir*, 1996, **12**, 788; (*b*) G. Schmid, Ed., *Clusters and Colloids*, VCH, New York, 1994; (*c*) M. M. Alvaiez, J. T. Khoury, T. G. Schaff, M. N. Shafigullin, I. Vezmar and R. L. Whetten, *J. Phys. Chem. B*, 1997, **101**, 3706; (*d*) A. P. Alivisatos, *J. Phys. Chem.*, 1996, **100**, 13226; (*e*) L. E. Brus, *Appl. Phys. A*, 1991, **53**, 465.
10 (*a*) A. Henglein, *J. Phys. Chem.*, 1993, **97**, 5457; (*b*) H. Weller, *Angew. Chem.*, *Int. Ed. Engl.*, 1993, **32**, 41; (*c*) H. Fendler and F. C. Meldrum, *Adv. Mater.*, 1995, **7**, 607.
11 H. Graber and M. H. Devoret, Eds., *Simple Charge Tunneling Coulomb Blockade Phenomena in Nanostructures*, NATO ASI Series B 294, Plenum, New York, 1992.
12 L. N. Lewis, *Chem. Rev.*, 1993, **93**, 2693.
13 (*a*) R. G. Freeman, K. C. Graber, K. J. Allison, R. M. Bright, J. A. Davis, A. P. Guthrie, M. B. Hommer, M. A. Jackson, P. C. Smith, D. G. Walter and M. J. Natan, *Science*, 1995, **267**, 1629; (*b*) G. Chumanov, K. Sokolov, B. W. Gregory and T. M. Cotton, *J. Phys. Chem.*, 1995, **99**, 9466.
14 T. Sato, D. Brown and F. G. Johnson, *Chem. Commun.*, 1997, 1007.
15 A. Doron, E. Katz and I. Willner, *Langmuir*, 1995, **11**, 1313.
16 M. Brust, D. Bethell, D. J. Schiffrin and C. J. Kiely, *Adv. Mater.*, 1995, **7**, 795.
17 R. Blonder, L. Sheeney and I. Willner, *Chem. Commun.*, 1998, 1393.
18 J. Schmitt, G. Decher, W. J. Dressick, S. L. Brandow, R. E. Geer, R. Shashidhar and J. M. Calvert, *Adv. Mater.*, 1997, **9**, 61.
19 U. Simon, G. Schön and G. Schmid, *Angew. Chem.*, *Int. Ed. Engl.*, 1993, **32**, 250.
20 (*a*) R. P. Andres, T. Bein, M. Dorogi, S. Feng, J. I. Henderson, C. P. Kubiak, W. Mahoney, R. G. Osifchin and R. Reifenberger, *Science*, 1996, **272**, 1323; (*b*) D. L. Klein, R. Roth, A. K. L. Lim, A. P. Alivisatos and P. L. McEuen, *Nature*, 1997, **389**, 699; (*c*) T. Sato and H. Ahmed, *Appl. Phys. Lett.*, 1997, **70**, 2759; (*d*) D. L. Feldheim and C. D. Keating, *Chem. Soc. Rev.*, 1998, **27**, 1; (*e*) T. Sato, H. Ahmed, D. Brown and B. F. G. Johnson, *J. Appl. Phys.*, 1997, **82**, 696; (*f*) D. L. Klein, P. L. McEuen, J. E. Bowen Katari, R. Roth and A. P. Alivisatos, *Appl. Phys. Lett.*, 1996, **68**, 2574.
21 M. Lahav, T. Gabriel, A. N. Shipway and I. Willner, *J. Am. Chem. Soc.*, 1999, **121**, 258.
22 A. N. Shipway, M. Lahav, R. Blonder and I. Willner, *Chem. Mater.*, 1999, **11**, 13.
23 (*a*) B. Odell, M. V. Reddington, A. M. Z. Slawin, N. Spencer, J. F. Stoddart and D. J. Williams, *Angew. Chem.*, *Int. Ed. Engl.*, 1998, **27**, 1547; (*b*) M. Asakawa, W. Dehaen, G. L'abbe, S. Menzer, J. Nouwen, F. M. Raymo, J. F. Stoddart and D. J. Williams, *J. Org. Chem.*, 1996, **61**, 9591.
24 J. Turkevich, P. C. Stevenson and J. Hiller, *Discuss. Faraday Soc.*, 1951, **11**, 55.
25 C. P. Collier, R. J. Saykally, J. J. Shiang, S. E. Henrichs and J. R. Heath, *Science*, 1997, **277**, 1978.
26 A. Doron, E. Joselevich, A. Schlittner and I. Willner, *Thin Solid Films*, 1999, **340**, 183.
27 (*a*) A. C. Benniston, A. Harriman, D. Philp and J. F. Stoddart, *J. Am. Chem. Soc.*, 1993, **115**, 5298; (*b*) T. T. Goodnow, M. V. Reddington, J. F. Stoddart and A. E. Kaifer, *J. Am. Chem. Soc.*, 1991, **113**, 4335; (*c*) E. Zahavy, M. Seiler, S. Marx-Tibbon, E. Joselevich, I. Willner, H. Dürr, D. O'Connor and A. Harriman, *Angew. Chem.*, *Int. Ed. Engl.*, 1995, **34**, 1005; (*d*) M. Kropf, E. Joselevich, H. Dürr and I. Willner, *J. Am. Chem. Soc.*, 1996, **118**, 655; (*e*) E. David, R. Born, E. Kaganer, E. Joselevich, H. Dürr and I. Willner, *J. Am. Chem. Soc.*, 1997, **119**, 7778.
28 M. Lahav, A. N. Shipway, I. Willner, M. B. Nielsen and J. F. Stoddart, submitted.
29 T. E. Young and B. W. Babbit, *J. Org. Chem.*, 1983, **48**, 562.

*Paper 9/02763G*